DETECTOR PERFORMANCE AND STABILITY OF THE CMS RPC SYSTEM DURING RUN 2

R. Hadjiiska[1,a]

on behalf of the CMS Collaboration

[1] *Bulgarian Academy of Sciences, Inst. for Nucl. Res. and Nucl. Energy,Tzarigradsko shaussee Boulevard 72, BG-1784 Sofia, Bulgaria*

E-mail: [a] roumyana.mileva.hadjiiska@cern.ch

The CMS (Compact Muon Solenoid) experiment, at the Large Hadron Collider (LHC) at CERN explores three different gaseous detector technologies in order to measure and trigger muons: CSC (Cathode Strip Chambers) in the forward regions, DT (Drift Tubes) in the central region, and RPC (Resistive Plate Chambers) both in the central and forward regions. The CMS RPC system provides information to all muon track finders and thus ensures the robustness and redundancy to the first level of muon triggering. Different approaches have been used to monitor the detector stability during the Run-2 data taking. The summary of the CMS RPC detector performance will be presented in terms of the main detector parameters — efficiency and cluster size, including the background measurements as well.

Keywords: Resistive-plate chambers, LHC

Roumyana Hadjiiska

1. Introduction

The second data taking period (Run-2) of LHC (Large Hadron Collider) held from 2015 till the end of 2018. During it LHC accelerated the proton beams up to energy of 6.5 TeV per beam resulting in collision energy of 13 TeV, almost near to the designed 14 TeV. The usual instantaneous luminosity was in order of 10^{34} $cm^{-2}s^{-1}$ reaching values up to 2 x 10^{34} $cm^{-2}s^{-1}$. Thanks to this, the total recorded integrated luminosity by CMS (Compact Muon Solenoid) detector collected in Run-1 and Run-2 is more than 177.65 fb^{-1}, providing valuable data for physics analyses and searches within and beyond the standard model of elementary particles.

A quadrant view of the CMS detector is shown in (Fig.1). The detector is composed by inner tracker system built of silicon strip and pixel layers, electromagnetic and hadron calorimetry system, installed inside the magnet and muon system, installed outside it. The CMS magnet provides a solenoidal magnetic field of 3.8 T inside the coil and 1.8 outside it. Detailed description of the CMS detector might be found in the literature [1]. Up to the end of Run-2, the CMS muon system explores three different gaseous detector technologies in order to ensure a proper measurement and triggering of the muons, born in the collisions. Both the barrel and endcap parts are built of four muon stations. DT (Drift Tube chambers) and CSC (Cathode Strip Chambers) are used for muon track reconstruction and muon pT measurements respectively in the barrel and endcap parts. The RPC (Resistive Plate Chambers) are installed both in the barrel and endcap and thus ensure the necessary redundancy of the muon system. There is one RPC layer per endcap station, resulting in four RPC layers in every of the endcaps. In the barrel, there are two RPC layers on the first and second stations and one layer per third and fourth one, resulting in total of six RPC barrel layers.

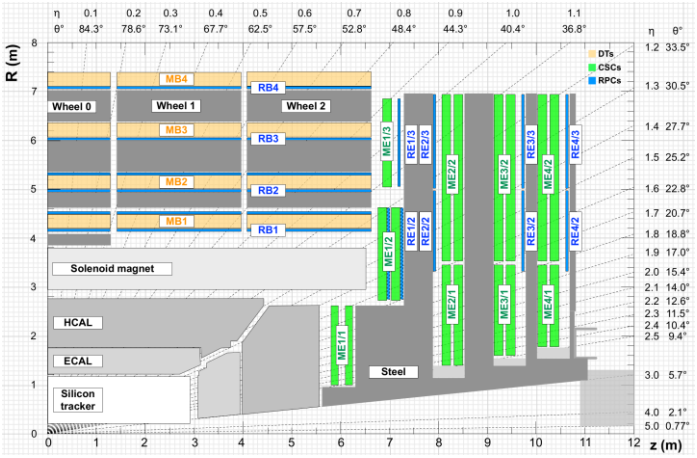

Figure 1. CMS quadrant – schematic view. The muon stations are labeled with MB (Muon Barrel) — Drift Tube chambers, ME (Muon endcap) — Cathode Strip Chambers and RB or RE for the Resistive Plate Chambers in the barrel and endcap respectively

The CMS trigger system explores two levels – the hardware L1 (Level One) trigger level and software algorithm level – so called HLT (High Level Trigger). During Run-1 the L1 trigger logic was based on the particular local triggers decisions from any of the sub-detectors. In order to cope with the drastically increased rate, in the beginning of the Run-2, L1 trigger has been re-based on a regional principle, collecting an input from all the detectors in a given pseudorapidity region in order to make its decision. Thus, the RPC system contributes to three different pseudorapidity regions relevant to BMTF, OMTF and EMTF (Barrel, Overlap and Endcap Muon Track Finders). The CMS RPCs explore double gap design with a common readout strips for both the gaps [2]. The space resolution is ~ 1 cm and the time resolution is ~2 ns [3]. The RPCs are used in CMS mainly as a trigger detector. They contribute to L1 mainly with hits as main trigger primitives. However, the existence of two RPC layers on the first and second barrel stations allows to build RPC segments and improve the trigger efficiency in the given region. The time window of the readout electronics is 25 ns. The fast time response ensure correct association of the measured particles with the collision time and relevant bunch crossing (BX). BX

association of the muon, coming from the proton-proton collisions measured in Run-2 are shown in (Fig.2). As might be seen from the plots (note the logarithmic Y scale) more than 99% of the measured muons are associated in the central BX window. Small fraction in the non-central BX windows are caused by background particles and post-collision effects.

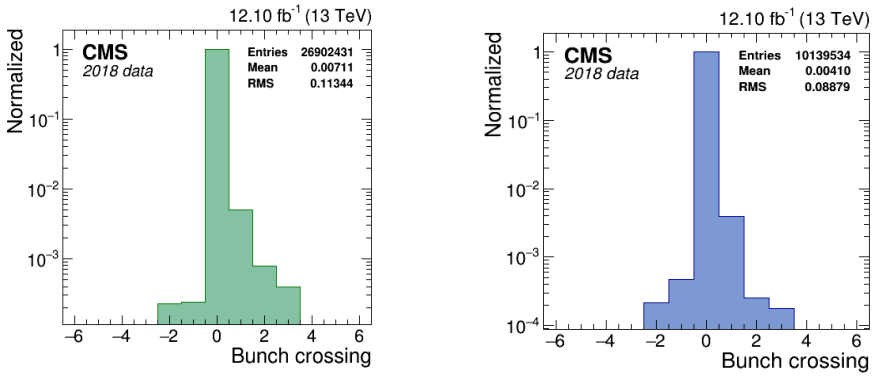

Figure 2. RPC BX distributions for RPC rechits from muons. Y axis is given in a logarithmic scale. The left plot represents barrel, while the one on the right — endcap

2. Background measurements

2.1 Methodology

Higher background levels can lead to lower performance in terms of detector efficiency, but it can lead also to detector ageing and shortening of its life or reduced operational capability. Therefore, measuring the background levels and permanent monitoring are very important.

According to the trigger logic, every RPC chamber is subdivided in two or three (in the barrel) and three (in the endcap) pseudorapidity partitions called rolls. Every barrel roll is connected to one link board (LB), while in the endcap, every three rolls from a given chamber are connected to one LB. The LB counts integrated over the run are normalized to time and active area of the strips in order to evaluate the RPC hit rate in [Hz cm^{-2}]. There are three main contributions - hits from collisions, hits caused from the radiation background and cosmics. There is also a small contribution from fake hits caused by the electronics, however their rate is negligible comparing to the total one. The linear dependence of the RPC hit rate on the instantaneous luminosity is well known [4] and used for permanent monitoring and predictions to higher luminosity scenarios [5]. However, their slopes depend on the background levels - as higher is the background, as steeper is the slope. This allows to study the non-uniformly distributed background in the cavern.

2.2 Barrel

RPC rates measured in the barrel vs instantaneous luminosity are shown in (Fig.3). The plot on the left represents the five barrel wheels, where W0 is the central one (closest to the interaction), and W+-2 are the outermost ones with respect the Z coordinate, where Z is measured along the beam pipe. Higher rates measured in W+-2 are caused mainly by the radiation leak from the HCAL gap (Fig 1), which affect mainly the first stations of the two external barrel wheels. The plot on the right represents barrel layers, where RB1in layer is installed at the lowest radius with respect to the beam line, and RB4 is at the largest. Highest rates measured in these layers are caused by two different components: in RB1 in - from prompt particles coming from collision and in RB4 – from the hits caused by the cavern background. The lowest rates are measured in W0 and the third barrel layer RB3, which are shielded by the other stations.

2.3 Endcap

RPC rates measured in the endcap station are shown in (Fig. 4). The plot on the left represent the linear dependence on the instantaneous luminosity, where RE+-1 depict for the innermost stations along beam pipe (Z coordinate) and RE+-4 for the outermost ones. Higher rate is measured in the outermost

forth stations, caused by the neutron induced cavern background. The rate is about 4 times higher with the respect the rates measured in the innermost edncap stations RE+-1.

The two plots on the right show the rate at a fixed luminosity of 1.5 x 10^{34} $cm^{-2}s^{-1}$ as functionof the azimuthal angle φ. A clear asymmetry is obvious –highest rate is measured in the top sectors (~90°) of the forth endcap stations, caused by the radiation leak from the gap in the rotating shielding of the beam pipe on the entrance of it in the cavern.

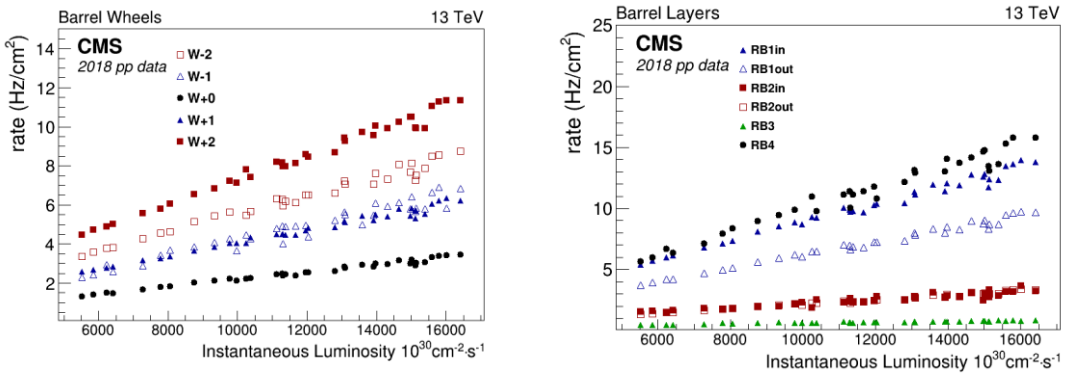

Figure 3. RPC hit rate as a function of the instantaneous luminosity, measured in proton-proton collision runs in 2018. Plot on the left, represents the five barrel wheels (at different Z positions along the beam pipe). Plot on the right represents barrel layers (different radii with respect to the beam pipe)

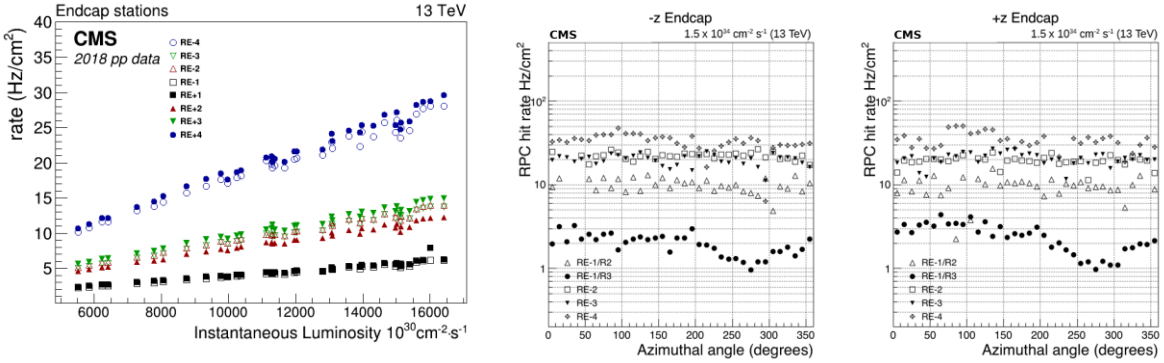

Figure 4. On the left - RPC hit rate, measured in the endcap stations (at different Z positions along the beam pipe) as a function of the instantaneous luminosity, measured in proton-proton collision runs in 2018. The two plots on the right show rates measured as a function of φ at fixed instantaneous luminosity

3. RPC detector performance

3.1 Main objects and monitored quantities

3.1.1 Cluster Size

There are many quantities which are carefully monitored on-line (during the time of the data taking) and offline (in the end of every particular data taking set). The main focus of the offline monitoring is on the cluster size and hit efficiency. The so called RPC rechits (reconstructed hits) are the output of the RPC local reconstruction and are built by the clustered adjacent strips, fired in the same BX window with response to the passing particles. The average cluster sizes range from 2 to 3 strips. The strip pitch is smaller for the RPCs installed at lower radii and larger for chambers on the outermost stations. Because of this the cluster size varies for the different RPC stations and it is larger for the innermost station RB1. The effect is well visible on the cluster size plot in (Fig.6).

3.1.1 Hit Efficiency

Two methods have been used to evaluate the RPC hit efficiency during Run-2.

• **Segment extrapolation method** [6] uses segments built in the nearest DT (in the barrel) or CSC (in the endcap) chambers. The segments are checked to belong to a standalone muon track (track built only in the muon system) and after than extrapolated to the RPC surface. The extrapolated points are matched to the points calculated from the RPC rechits in a range as much as four strips. The efficiency is calculated as a ratio between the number of the matched hits and the number of extrapolations. This is the main method used for daily monitoring both in Run-1 and Run-2. The same is used also for the RPC HV WP (High Voltage Working Point) calibration. However with a drastic increase of the instantaneous luminosity in the beginning of Run-2, it was found a small dependence of the method on the instantaneous luminosity, caused by an increase of fake tracks with low quality. Because of this the method was tuned, requiring better quality (chi2/ndof < 8 and p_T > 7 GeV) for the muon track under study.

• **Tag & Probe** (T&P) method [7] - explores two independent muon identification algorithms – Tracker muon (inner tracker track, tagged as muon by the DT/CSC segments) and RPCMuon (inner tracker track, tagged as muon in the the RPC hit). The muons from the two samples have been checked to pass relevant criteria to form a Z→ μμ resonance. The method was accepted as a main for the RPC efficiency measurements in the end of Run-2. The usage of physics trigger suppresses an algorithm dependence on the instantaneous luminosity. However it is statistically dependent and require higher statistics in order to have enough Z→μμ events. Because of this the presented results (Fig.5) are averaged over all the events in a given LHC fill.

3.2 Performance stability

3.2.1 Performance history

The history of the RPC barrel detector performance during Run-2 is presented in (Fig.5). Hit efficiency and cluster size are plotted as a function on the integrated luminosity in order to monitor for potential ageing effects. The vertical red lines represent the planned short technical stops during data taking, and the black – the end of year technical stops. The trend of the curves follows the changes of the applied high voltage working points and changes of the Isobutane concentration in the working gas mixture, explained in [8]. The drop of the efficiency in Aug. 2018 (at ~110 fb^{-1}) is caused by a known configuration setting problem, spotted by the offline monitoring and corrected after that. Similar results are obtained also for the endcap parts. No degradation effects of terms of inefficiency are observed with an increase of the instantaneous luminosity, however slight dependence on the background levels is observed. As might be seen from the same plot, the lowest efficiency is measured for the outermost forth station (RB4) where the measured background rate is highest comparing the other barrel muon stations (Fig. 3).

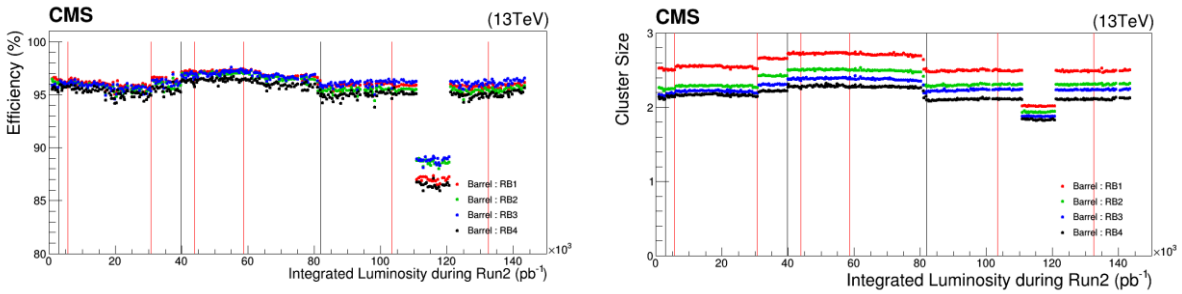

Figure 5. RPC efficiency and cluster size history vs integrated luminosity for the four barrel stations: The plots represent Run-2 history. (Run-1 integrated luminosity is 27 fb^{-1}). Each point corresponds to an average efficiency or cluster size per station in a given LHC fill

3.2.1 Overall comparison

The plots in (Fig. 6) show a comparison between the RPC overall efficiency measured during the years of Run-2 (2015-2018). The plot on the left depicts the barrel, and the one on the right - the endcap rolls. The underflow entries are from rolls with efficiency lower than 70%, caused by known

hardware problems - threshold control, chambers switched off because of gas leak problems. The numbers given on the plots show the average efficiency for the well performing and the fraction of the problematic RPC rolls. The RPC efficiencies measured in 2015-2018 are comparable and in agreement with the design requirements of efficiency above 95%.

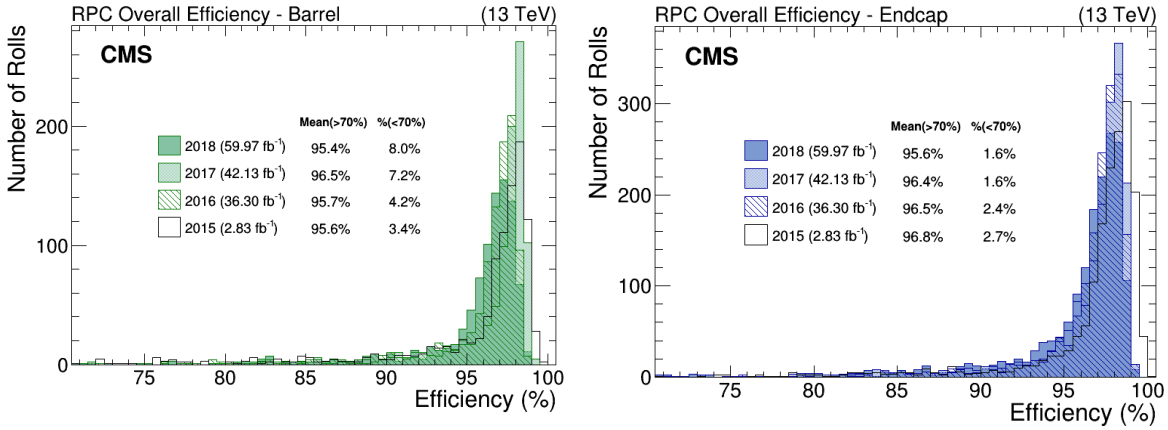

Figure 6. Overall efficiency distribution of RPC rolls during the LHC Run-2 (2015-2018) for barrel (left) and endcap (right) region. The underflow entries are from rolls with efficiency lower than 70%, caused by known hardware problems - threshold control, chambers switched off because of the gas leak problems. The numbers given on the plots show the average efficiency for the well performing and the fraction of the problematic RPC rolls. The RPC efficiencies measured in 2015-2018 are comparable and in agreement with the expectations

4. Conclusion

The CMS RPC detector performance has been studied in terms of background rate, hit efficiency and cluster size with proton-proton collision data at collision energy 13 TeV and instantaneous luminosity ~10^{34} $cm^{-2}s^{-1}$ during all the years of LHC Run-2 (2015-2018). The efficiency estimation algorithms have been tuned properly in order to cope with the increase of the instantaneous luminosity. A slight but obvious dependence on the background levels is observed, resulting in a small efficiency decrease with increase of the background caused rate. The operational problems were well understood and compensated with proper calibrations. The RPC detector performance is stable, facing the designed requirements.

5. Acknowledgment

We would like to thank all our colleagues from the CMS RPC group for their dedicated work to keep the stable performance of the RPC system. We wish to congratulate our colleagues in the CERN accelerator departments for the excellent performance of the LHC machine. We thank the technical and administrative staff at CERN and all CMS institutes.

References

[1] CMS Collaboration, The CMS experiment at the CERN LHC, JINST 3 S08004 (2008)

[2] CMS Collaboration, The CMS muon project: Technical Design Report. 1997. CERN-LHCC-97-032, CMS-TDR-003

[3] M. Abbrescia et al., Beam test results on double-gap resistive plate chambers proposed for CMS experiment, Nucl. Instr. Meth. A 414 (1998) 135–148

[4] S. Costantini et al.,Radiation background with the CMS RPCs at the LHC, 2015 JINST 10 C05031, [arXiv:1406.2859]

[5] R.I. Rabadan-Trejo et al., Long-term performance and longevity studies ofthe CMS Resistive Plate Chambers, 2018 JINST 13 P08024

[6] CMS Collaboration, Performance of CMS muon reconstruction in pp collision events at √s=7TeV, 2012 JINST 7 P10002, [arXiv:1206.4071]

[7] J. Goh *et al, CMS RPC efficiency measurement using the tag-and-probe method*, 2019 *JINST* **14** C10020

[8] M. A. Shah et al (CMS Collaboration), The CMS RPC Detector Performance and Stability during LHC RUN-2, 2019 JINST 14 C11012, [arXiv:1808.10488]